Cement and Concrete Research 78 (2015) 190–199

Contents lists available at ScienceDirect

Cement and Concrete Research

journal homepage: http://ees.elsevier.com/CEMCON/default.asp

# Determination of the chloride diffusion coefficient in blended cement mortars

V. Elfmarkova [a,*], P. Spiesz [a,b], H.J.H. Brouwers [a]

[a] Department of the Built Environment Eindhoven University of Technology, P. O. Box 513, 5600 MB Eindhoven, The Netherlands
[b] ENCI HeidelbergCement Benelux, The Netherlands

ARTICLE INFO

*Article history:*
Received 28 July 2014
Accepted 9 June 2015
Available online 23 August 2015

*Keywords:*
Diffusion (C)
Chloride (D)
Blended cement (D)
Mortar (E)
Transport properties (C)

ABSTRACT

The rapid chloride migration test (RCM) is a commonly used accelerated test for the determination of the chloride diffusion coefficient in concrete. Nevertheless, the initial development and further experience with the RCM test concern mainly the ordinary Portland cement system. Therefore, the objective of this work is to analyse the application of this test method for other types of binders, by performing and analysing the RCM test results for mortars prepared with additions of supplementary cementitious materials. A comparison is given between the total chloride concentration profiles measured in concrete after the RCM test and the colourimetric test results. The presented results show that the accuracy of the silver nitrate colourimetric technique is sufficient for the determination of the chloride penetration front and that the RCM test is a suitable method also for the determination of chloride diffusion coefficient in mortars with blended cements.



## 1. Introduction

The key performance requirements for the design, construction and maintenance of concrete structures are related to safety, serviceability and durability. The highly alkaline environment of concrete forms a passive film on the surface of steel bars, which normally prevents the steel from corrosion. However, under chloride attack, the passive film vanishes and the steel spontaneously corrodes. Chloride-induced corrosion of reinforcing steel occurs in chloride-bearing environments (e.g. sea water, de-icing salts) and is directly related to the shortened service life of concrete structures/elements. In order to quantify the chloride ingress speed in concrete, the chloride diffusion coefficient is used, because the diffusion controls the ingress of chlorides at a certain depth in concrete, while the capillary suction is only significant in the surface layers [1,2].

Several laboratory test methods are being commonly used for determining the chloride diffusion coefficient. The bulk immersion tests, described e.g. in NT Build 443 [3] or ASTM C1556–03 [4], are long term diffusion tests in which concrete samples are exposed to a chloride solution for a relatively long period of time. However, the long term methods are often not preferred in practice because they are time consuming and laborious. The rapid chloride migration (RCM) test developed by Tang [5], described in the guideline NT Build 492 [6], is one of the accelerated test methods in which chlorides penetrate the concrete at high rates due to the applied electric field. The output of the test is the chloride diffusion coefficient $D_{RCM}$ (often called the migration coefficient — to distinguish it from immersion tests). This method is concluded by some researchers to be the most suitable of all the reviewed accelerated chloride tests, on the basis of its simplicity, short duration and often is assumed to have a clear theoretical basis [7]. In the RCM test, after a period of the application of electric field to concrete, the chloride penetration depth in a split concrete sample is measured by an easy and quick $AgNO_3$ colourimetric method (0.1 $mol \cdot dm^{-3}$ $AgNO_3$ solution sprayed onto the fractured concrete surface). The $AgNO_3$ colourimetric method involves two parameters — the indicated chloride penetration depth $x_d$ and the free-chloride concentration $c_d$ at which the colour change occurs in concrete. Both these values are used to calculate the non-steady-state diffusion coefficient of chloride ($D_{RCM}$). The $D_{RCM}$ is obtained from the following mathematical model [5]:

$$\frac{\partial c}{\partial t} = -\frac{\partial J_x}{\partial x} = \frac{D_0}{1+\frac{\partial c_b}{\partial c}}\left(\frac{\partial^2 c}{\partial x^2} - \frac{zFE}{RT}\cdot\frac{\partial c}{\partial x}\right) = D_{RCM}\left(\frac{\partial^2 c}{\partial x^2} - \frac{zFE}{RT}\cdot\frac{\partial c}{\partial x}\right). \quad (1)$$

A solution of this model is presented in [5] and yields the following equation for the $D_{RCM}$:

$$D_{RCM} = \frac{RT}{zFE}\cdot\frac{x_d - \alpha\sqrt{x_d}}{t} \quad (2)$$

where: c — concentration of free-chlorides in pore solution, t — time, $J_x$ — total flux of chlorides in x direction, x — distance, $D_0$ — intrinsic chloride diffusion coefficient in pore solution of concrete, $c_b$ —

* Corresponding author. Tel.: +31 0 40 247 5469; fax: +31 0 40 243 8595.
*E-mail address:* elf.veronika@gmail.com (V. Elfmarkova).

http://dx.doi.org/10.1016/j.cemconres.2015.06.014
0008-8846/

concentration of bound chlorides, E — electric field, equal to $(U-2)/L$, where U — applied electrical voltage and L — thickness of sample (0.05 m), R — gas constant (8.314 $J \cdot mol^{-1} \cdot K^{-1}$), T — temperature (293 K), z — ion valence (−1 for $Cl^-$), F — Faraday constant (96,485 $C \cdot mol^{-1}$), $x_d$ — chloride penetration depth indicated by the colourimetric indicator $AgNO_3$, α — laboratory constant defined as [5]:

$$\alpha = 2\sqrt{\frac{RT}{zFE} \cdot erf^{-1}\left(1-\frac{2c_d}{c_0}\right)} \quad (3)$$

where: $c_d$ — free-chloride concentration at colour change boundary (0.07 $mol_{Cl}/dm^3_{solution}$) and $c_0$ — concentration of chlorides in the external bulk solution (64.95 $g_{Cl}/dm^3_{solution}$ = 1.83 $mol_{Cl}/dm^3_{solution}$).

As previously stated, the free chloride penetration depth $x_d$ is used for the calculation of the $D_{RCM}$ according to Eq. (2) and it is determined using the $AgNO_3$ solution. Spraying the silver nitrate solution onto a freshly fractured concrete cross-section leads to a chemical reaction which results in a clear colour change boundary between the chloride-contaminated and chloride free-zones. This is due to the fact that in the regions not containing chloride ions, $AgNO_3$ reacts with $OH^-$ to form a mixture of precipitates of silver hydroxide, according to Eq. (5). The precipitates of AgOH formed on the surface are unstable and quickly decompose to a brownish precipitate ($Ag_2O$) [8–10]. The zone containing chlorides is indicated by a white precipitate resulting from formation of silver chloride (AgCl), as Eq. (4) shows. The chemical reactions can be expressed as follows [9]:

$$Ag^+ + Cl^- \rightarrow AgCl\downarrow (\text{silvery white colour} = 100\%\, AgCl + 0\%\, Ag_2O) \quad (4)$$

$$Ag^+ + OH^- \rightarrow AgOH \rightarrow Ag_2O\downarrow (\text{browncolour} = 0\%\, AgCl + 100\%\, Ag_2O) \quad (5)$$

Otsuki et al. [10] found that 0.1 M $AgNO_3$ solution is the most appropriate concentration for giving the visually clearest boundary between the chloride- and chloride-free zones in the case of OPC. From the data reported in the literature [8–13] it is known that the total chloride content at the colour change boundary detected by silver nitrate varies in a wide range, from 0.19% [14] to 1.41% [11] by the mass of ordinary Portland cement, and from 0.02% [11] to 0.5% [10] by mass of concrete, depending on the sample preparation and the measurement technique. Nevertheless, this concentration of $AgNO_3$ may be different for other binders due to the differences in chloride binding, hydration products, or pore solution chemical composition and therefore, may not be suitable for all types of concrete [5,8–13,15,16]. Yuan [14] reported some difficulties with the accuracy of the chloride penetration depth measurement in concrete after using the $AgNO_3$ solution as a chloride indicator. Moreover, the free-chloride concentration at the colour change boundary of 0.07 $mol \cdot dm^{-3}$ was questioned in [14]. Such value was proposed by Tang [5,17], based on the experiments of Otsuki et al. [10], and applied for the $D_{RCM}$ calculation. Otsuki et al. [10] found a free chloride concentration at the colour change boundary of approximately 0.14 $mol \cdot dm^{-3}$. Tang [5,17] used value of 0.07 $mol \cdot dm^{-3}$ considering a chloride condensation factor of 2 due to the pore solution extraction technique. However, this concentration may be different for blended cements, which has been experimentally confirmed by Maes et al. [15], who reported the chloride concentration at the colour change boundary of 0.35 $mol \cdot dm^{-3}$ for concretes based on OPC–GGBS blends. This is in line with [18,19], which suggest that mineral additions may influence the chloride concentration at the colour change boundary.

Many researchers have shown that the chloride profiles determined experimentally after performing the RCM test have significantly different shape compared to the theoretical profile shape predicted from Eq. (1) [14,16,20]. The difference between the theory and experimental measurements gives an evidence that the basic chloride transport model for the RCM test unsatisfactorily describes the real process. Tang [5] suggested the possible explanations for the differences between the theoretical and experimental chloride concentration profiles, such as (a) different pore distribution resulting in different penetration front; (b) reaction kinetics which changes the shape of the profile without changing the penetration depth or (c) influence of other ions on the chloride binding [5]. Recently, Šavija et al. [21] attributed the discrepancy between the theoretical and experimental chloride profiles to the tortuosity of the pore structure and heterogenity of concrete, yet without considering chloride binding in the simulations. As explained in [16,20,22] the oversimplification of chloride binding in the transport model can explain the observed discrepancies. Eq. (1) assumes a constant $\partial c_b/\partial c$ term, which implicitly implies that either no binding or an instantaneous linear chloride binding in equilibrium is present in concrete. For the linear chloride binding in instantaneous equilibrium, the free-chloride concentration would be reduced in concrete by binding, but the shape of the free-chloride concentration profile would remain unaffected (i.e. the abrupt chloride profile, instead of the gradual profile, as experimentally determined after the test). Therefore, Spiesz et al. [16,23] presented an extended chloride transport model which considers chloride binding more properly, assuming a non-linear chloride binding isotherm (represented by Freundlich isotherm $C_b = K_b \cdot c^n$) and non-equilibrium conditions between the free and bound chlorides. This

**Table 1**
Specific densities ($\rho_s$) of used materials.

| Material | $\rho_s$ [g · cm$^{-3}$] |
|---|---|
| CEM I 52.5 N | 3.19 |
| GGBS | 2.91 |
| FA | 2.36 |
| SF | 2.25 |
| Sand 0–4 mm | 2.65 |
| SP | 1.10 |

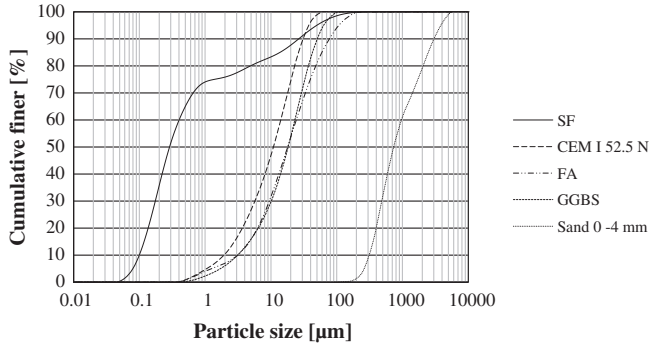


**Fig. 1.** Particle size distribution of the used materials.

**Table 2**
Chemical composition of OPC, GGBS, FA and SF.

| Chemical composition [%] | OPC | GGBS | FA | SF |
|---|---|---|---|---|
| CaO | 64.60 | 38.89 | 4.46 | 0.28 |
| $SiO_2$ | 20.08 | 34.18 | 55.32 | 94.25 |
| $Al_2O_3$ | 4.98 | 13.63 | 22.45 | 0.96 |
| $Fe_2O_3$ | 3.24 | 0.51 | 8.52 | 0.14 |
| $K_2O$ | 0.53 | 0.43 | 2.26 | 0.95 |
| $Na_2O$ | 0.27 | 0.33 | 1.65 | 0.18 |
| $SO_3$ | 3.13 | 1.41 | 1.39 | – |
| MgO | 1.98 | 10.62 | 1.89 | 0.40 |
| $TiO_2$ | 0.30 | – | 1.17 | 0.01 |
| $Mn_3O_4$ | 0.10 | – | 0.11 | – |
| $P_2O_5$ | 0.74 | – | 0.76 | 0.08 |

**Table 3**
Composition of the developed mortar mixtures.

| Name of mix | M1-OPC | | M2-GGBS | | M3-FA | | M4-SF | |
|---|---|---|---|---|---|---|---|---|
| Material | Volume [dm$^3$] | Mass [kg·m$^{-3}$] | Volume [dm$^3$] | Mass [kg·m$^{-3}$] | Volume [dm$^3$] | Mass [kg·m$^{-3}$] | Volume [dm$^3$] | Mass [kg·m$^{-3}$] |
| CEM I 52.5 N | 163.2 | 520.6 | 97.9 | 312.3 | 138.7 | 442.5 | 146.9 | 468.5 |
| GGBS | 0.0 | 0.0 | 71.6 | 208.2 | 0.0 | 0.0 | 0.0 | 0.0 |
| FA | 0.0 | 0.0 | 0.0 | 0.0 | 33.1 | 78.1 | 0.0 | 0.0 |
| SF | 0.0 | 0.0 | 0.0 | 0.0 | 0.0 | 0.0 | 23.1 | 52.1 |
| Sand 0–4 mm | 594.0 | 1574.1 | 594.0 | 1574.1 | 594.0 | 1574.1 | 594.0 | 1574.1 |
| Water | 208.3 | 208.3 | 208.3 | 208.3 | 208.3 | 208.3 | 208.3 | 208.3 |
| SP (% bwob) | – | 0.4% | – | 0.2% | – | 0.4% | – | 0.4% |
| Estimated air content | 30.0 | 3.0% | 30.0 | 3.0% | 30.0 | 3.0% | 30.0 | 3.0% |
| Total | 995.5 | 2303.0 | 1001.8 | 2303.0 | 1004.2 | 2303.0 | 1002.4 | 2303.0 |

model is based on the simplified Nernst–Planck equation in transient conditions, coupled with a reaction term, and reads as follows [16]:

$$\phi\frac{\partial c}{\partial t}-D_{eff}\left(\frac{\partial^2 c}{\partial x^2}-\frac{zFU}{RTL}\cdot\frac{\partial c}{\partial x}\right)=-k\left[c-\left(\frac{C_b}{K_b}\right)^{1/n}\right] \tag{6}$$

$$(1-\phi)\rho_s\frac{\partial C_b}{\partial t}=k\left[c-\left(\frac{C_b}{K_b}\right)^{1/n}\right] \tag{7}$$

with the following boundary and initial conditions:

$$c(x=0;t)=c_0 \tag{8}$$

$$C_b(x;t=0)=C_{bi}$$

where: $D_{eff}$ — effective chloride diffusion coefficient, k — mass transfer coefficient, $K_b$ — binding capacity of concrete, n — binding intensity parameter, $C_b$ — bound chloride concentration expressed per mass of concrete, φ — water-permeable porosity concrete, $\rho_s$ — specific density of concrete and $C_{bi}$ — initial bound chloride concentration in concrete.

The study of Spiesz and Brouwers [23] has shown that the $D_{RCM}$, as determined from Eqs. (1)–(3) for OPC-based concretes is not affected by chloride binding and therefore the test output is correct for OPC-based concretes. It is owed to fact that $AgNO_3$ colourimetric method was found reliable the detection of the free chloride penetration front in the OPC-based concrete. It has been demonstrated that the chloride binding capacity is very low at low free-chloride concentrations during migration test ($\partial c_b/\partial c \approx 0$ in Eq. (1)) and hence, the progress of the free-chloride penetration front through the concrete sample is not retarded by chloride binding. Therefore, since in the migration tests chloride binding can be neglected at very low free chloride concentrations, the $D_{RCM}$ calculated from the detected free chloride penetration front remains unaffected in the OPC-based systems. Thus, the $D_{RCM}$ formula shown in Eq. (1) can be modified by neglecting the chloride binding capacity and an equation has been suggested in [22], based on the equation presented by Atkinson and Nickerson [24]:

$$D_{RCM}=\frac{D_0}{1+\frac{\partial c_b}{\partial c}}=\frac{D_{eff}}{\phi\left(1+\frac{\partial c_b}{\partial c}\right)}\approx\frac{D_{eff}}{\phi}. \tag{9}$$

Nevertheless, for blended cements the validity of Eq. (9) and of the $D_{RCM}$ (Eq. (2)) has not been analysed yet and hence, the suitability of the $AgNO_3$ colourimetric method to accurately detect the free-chloride penetration front in concrete based on different types of binder should be verified.

Therefore, the purpose of this study is to analyse the accuracy of the determination of the chloride diffusion coefficient in the RCM test for various blended cement mortars. The diffusion coefficients are obtained by two approaches: the basic RCM test model (Eqs. (1)–(3)) [5,6] and the extended model presented by Spiesz et al. (Eqs. (6)–(8)) [16,23]. Firstly, the total concentrations of chlorides at the $AgNO_3$ colour change boundary are determined in mortars with different binders. Then, the $D_{RCM}$ obtained from the basic model is compared to the one derived from the extended model. Furthermore, the apparent chloride diffusion coefficient obtained in long-term immersion test is estimated in order to demonstrate the influence of blended cements on the chloride transport properties of mortars and the RCM test reliability.

## 2. Materials and methods

### 2.1. Materials and mix design

In this study four mortars based on different binder blends were prepared and tested. For a better results' clarity mortars were chosen instead of concrete as they did not contain coarse aggregates, which are

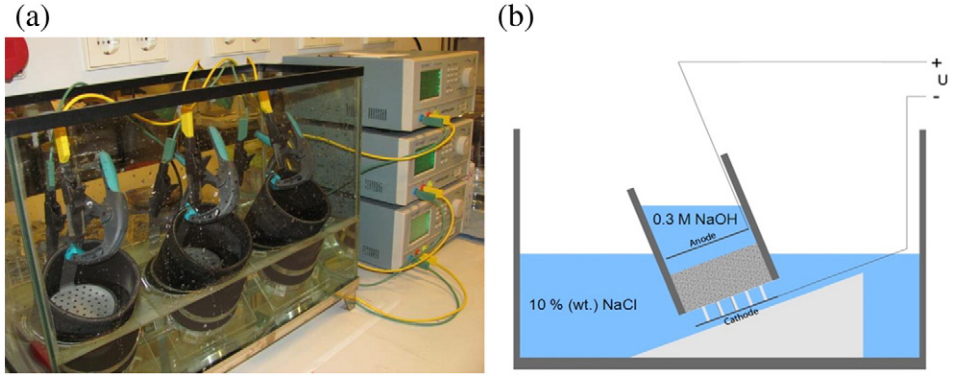


**Fig. 2.** Rapid chloride migration test set-up (a) and scheme [28] (b).

impermeable to chlorides and therefore disturb the chloride penetration front. The reference mortar consisted of ordinary Portland cement (CEM I 52.5 N) as a binder. The other mixtures included OPC replaced at different levels by supplementary cementitious materials (SCM) — ground granulated blast-furnace slag (GGBS), fly ash (FA) and silica fume (SF). The binders were prepared by blending OPC with GGBS, FA and SF to achieve the same composition as specified for CEM III/A, CEM II/A–V and CEM II/A–D in EN 197-1 [26]. The water/binder ratio was kept constant for all the prepared mixes (w/b = 0.4). Sand 0–4 mm was used as aggregate. The workability of the mortars was adjusted with superplasticizer (Glenium 51 (BASF)). The granulometric properties are shown in Fig. 1 and densities and chemical compositions of used materials are shown in Tables 1 and 2, respectively. The mixture proportions of the prepared mortars are shown in Table 3.

Fresh mortars were cast in cubes (150 mm side length) and prisms ($40 \times 40 \times 160$ mm$^3$). One day after casting, the specimens were demolded and cured in water until the age of 27 days, when the RCM test samples and long-term diffusion test samples were extracted from the cubes by drilling and cutting. At the age of 28 days the RCM test (NT Build 492) and long-term diffusion test (NT Build 443) began. Mortar prisms were used for the determination of flexural and compressive strengths according to EN 196–1 [27], after 7, 28 and 91 days of water curing.

### 2.2. Rapid chloride migration test (RCM)

The cylinders were firstly drilled from cubes and cut to the required thicknesses. Cylindrical samples of 100 mm diameter and 50 mm thickness were used in the tests. The test samples were saturated with limewater under vacuum conditions, following the procedure specified in [6]. A pressure of about 20 mbar was applied to the samples in the desiccator for three hours, and then, with the vacuum pump still running, the desiccator was filled with limewater. The vacuum was maintained for an additional hour before allowing air to slowly re-enter the desiccator. The specimens were stored in the solution for $18 \pm 2$ h prior to the test RCM test. Subsequently, the samples were placed in tightly clamped rubber sleeves, as is shown in Fig. 2 [28]. The catholyte was a 10% NaCl solution and the anolyte 0.3 M NaOH solution. The test duration and applied voltages were determined based on the initial current measured at 30 V [6]. The RCM test duration for all the investigated mortar mixes was 24 h and the applied voltages are shown in Table 6. The RCM test was carried out on six cylindrical samples per each mortar type. At the end of the test, three cylinders were split and sprayed with 0.1 M $AgNO_3$ solution in order to determine the penetration depth of chlorides, while the total chloride concentration profiles were measured in the other three samples as it is explained in Section 2.4. Finally, the $D_{RCM}$ was calculated from Eqs. (2) and (3). The measured profiles were then used to estimate the chloride diffusion coefficient based on the extended chloride migration model presented in Eqs. (6) and (7).

### 2.3. Chloride diffusion test

The chloride diffusion coefficient was also determined here using the long-term bulk immersion tests (NT Build 443 [3]). The test was carried out on triplicate specimens. Cylindrical specimens (drilled from 150 mm cubes) with a diameter of 100 mm and a thickness of 50 mm were used. At the age of 28 days, all faces of the cylinders except the one exposed to chloride solution were coated with an epoxy resin and immersed in limewater until the mass of the samples stabilized. Subsequently, the saline solution was prepared, 165 g of NaCl per dm$^3$, and the samples were exposed to this environment. The containers with the samples were shaken once every week. After each five weeks, the exposure liquid was replaced with a fresh solution. After the immersion period of 120 days, the specimens were removed from the solution. One specimen was split for the determination of the chloride penetration depth by spraying $AgNO_3$ solution. The chloride concentration profiles were measured in the two remaining specimens immediately after the exposure period, by grinding off material layers and determining their total chloride content. The powder collected from each layer was dried at 105 °C until a constant mass was reached. Subsequently, the total chloride concentration was determined by the potentiometric titration method as will be presented in Section 2.4. The diffusion coefficient was obtained by fitting the measured profile to the solution of the 2nd Fick's law, as described in NT Build 443 [3].

**Table 4**
Fresh state properties of mortar mixes; $\rho_f$ — density of mortar in fresh state, $V_{air,calc}$ — calculated entrapped air volume.

| Mixture | $\rho_f$ [kg·m$^{-3}$] | Slump [mm] | Flow [mm] | $V_{air,calc}$ [%] |
|---|---|---|---|---|
| M1-OPC | 2210 | 20 | 155.0 | 7.7 |
| M2-GGBS | 2160 | 10 | 132.5 | 9.8 |
| M3-FA | 2200 | 20 | 155.0 | 7.6 |
| M4-SF | 2150 | 20 | 145.0 | 10.2 |

### 2.4. Determination of the total chloride concentration

After performing the RCM test and long-term diffusion test, the mortar specimens were ground to powder in layers. A surface layer of 0.5 mm was ground first and then 1.0 mm layers were ground subsequently, until a depth was achieved approximately 4 mm deeper than the chloride penetration depth measured previously on sister samples (by $AgNO_3$ colorimetric method). The powder collected from each layer was dried at 105 °C until a constant mass was reached. The total chloride concentration was determined by boiling 2 g of the powder in 35 ml distilled water acidified with 2 ml of 1.0 M $HNO_3$. After boiling, the solution was cooled down and then filtered. Subsequently, the volume of the filtered solution was adjusted to 100 ml by adding distilled water. Samples of 10 ml were analysed for the chloride concentration by using an automatic potentiometric titration unit and a 0.01 M $AgNO_3$ solution as a titrant. The measured concentration is expressed as the mass of chlorides in 100 g of dry mortar (% $m_{Cl}/m_{sample}$).

### 2.5. Additional measurements

The water-permeable porosity of mortar samples was measured on five cylindrical samples for each mixture, extracted from 150 mm cubes. The discs of 100 mm diameter and about 15 mm height were firstly water-saturated under vacuum conditions at the age of 28 days, following the same procedure as described earlier in Section 2.2. After completing the saturation, the mass of the discs was measured hydrostatically and in air. Subsequently, the samples were oven-dried at 105 °C until a constant mass was reached. Finally, the water-permeable porosity $\phi$ is calculated as follows [29]:

$$\phi = \frac{m_s - m_d}{m_s - m_w} \cdot 100 \quad [\%], \tag{10}$$

where $m_s$ — mass of saturated sample measured in air, $m_w$ — mass of saturated sample measured hydrostatically and $m_d$ — mass of dried sample.

**Table 5**
Hardened state properties of mortar mixes after 28 days; $R_{t,28}$ — flexural strength, $R_{c,28}$ — compressive strength, $\phi_{28}$ — porosity, $\rho_d$ — density of mortar in dry state.

| Mixture | $\rho_d$ [kg · m$^{-3}$] | | $R_{t,28}$ [N · mm$^{-2}$] | | $R_{c,28}$ [N · mm$^{-2}$] | | $\phi_{28}$ [%] | |
|---|---|---|---|---|---|---|---|---|
| | Average | StDev | Average | StDev | Average | StDev | Average | StDev |
| M1-OPC | 1830 | 0.13 | 9.2 | 0.17 | 60.4 | 3.46 | 14.64 | 0.28 |
| M2-GGBS | 1960 | 0.06 | 7.8 | 0.01 | 51.9 | 1.68 | 14.67 | 0.24 |
| M3-FA | 2000 | 0.52 | 7.3 | 0.15 | 54.0 | 1.18 | 17.42 | 0.46 |
| M4-SF | 1930 | 0.37 | 7.9 | 0.02 | 59.3 | 2.22 | 17.85 | 0.70 |

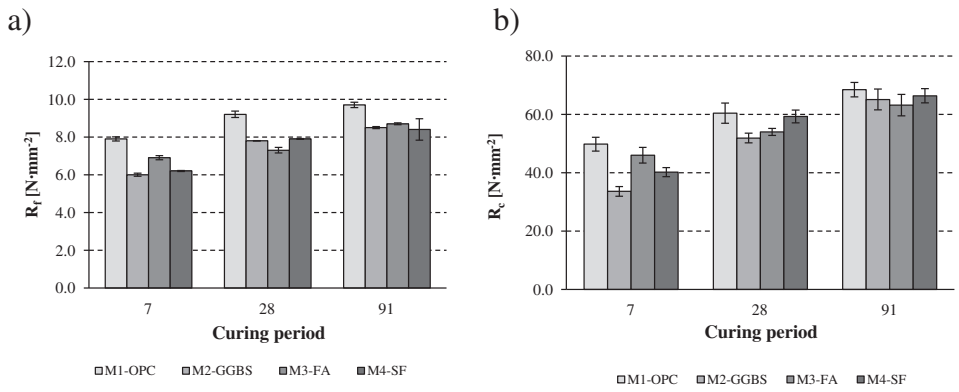


**Fig. 3.** Development of flexural (a) and compressive (b) strengths of mortars mixes after 7, 28 and 91 days.

## 3. Results and discussion

### 3.1. Fresh state properties

The slump of mortars was measured with a small Abrams cone and the flowability with a Hägermann cone. The target slump for all the mixtures was set to 10–20 mm and the flowability > 130 mm and adjusted by adding superplasticizer. Table 4 presents the fresh state properties of the mortars. The entrapped air volume in the mortars was estimated from the difference between the designed and measured density. It can be observed that the mortar M4-SF has a higher air content compared to the other mixtures. This can be attributed to a higher viscosity of mortar resulting from the application of silica fume, which has a high specific surface area [30,31]. The increased air content in mortar M2-GGBS can be attributed to its lower workability, caused by a lower SP dosage compared to the other mixtures (see Table 3).

### 3.2. Hardened state properties

Table 5 gives an overview of the determined hardened properties of the prepared mortars. The compressive and flexural strengths development (up to 91 days of curing) is presented in Fig. 3, from which it can be noticed that the OPC-based mortar develops the highest strengths among the prepared mortars. The results show that the mortar M4-SF has the highest permeable porosity (17.85%) compared to the other mortars. The measured water-permeable porosity accounts for the closed pores (entrapped air) and the capillary porosity. The capillary porosity is normally reduced when pozzolanic materials are added [32]. Nevertheless, the air entrapped in the fresh mix influences the total porosity, so that it does not necessarily decrease when SCM are incorporated, even though the capillary porosity can be reduced. This has been demonstrated by Quercia et al. [30] who found that nano-silica additions into concrete can even increase the total concrete porosity compared to the reference samples, but at the same time reduce the capillary porosity, i.e. hinder the chloride transport in concrete.

### 3.3. Chloride penetration depth and $D_{RCM}$

After performing the RCM test, the colourimetric indicator for chlorides ($AgNO_3$ solution) is sprayed onto freshly split mortar samples to determine the chloride penetration depth. The colourimetric boundary between the regions with and without chlorides is clearly visible due to the chemical reaction of $Ag^+$ with $Cl^-$ or $OH^-$ and formation of white or dark precipitate regions as illustrated in Fig. 4. The difficulty

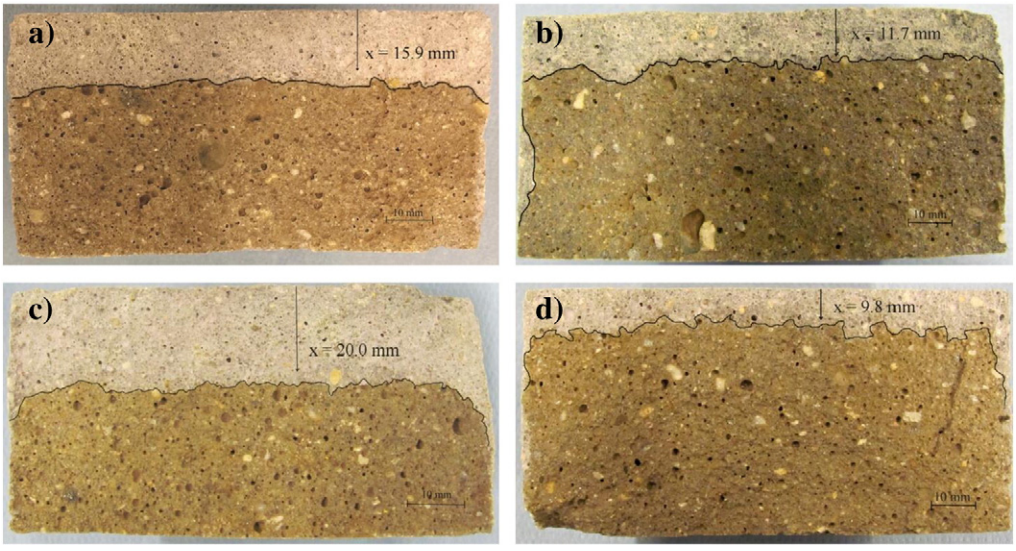


**Fig. 4.** Examples of the chloride penetration depth indicated by $AgNO_3$ solution sprayed onto freshly split mortar samples after the RCM test — a) M1-OPC1; b) M2-GGBS1; c) M3-FA2; d) M4-SF2.

**Table 6**
RCM test conditions and results.

| Mortar mixture | Sample | Applied voltage [V] | Initial current (30 V) [mA] | Test duration [h] | $x_d$ [mm] | $D_{RCM}$ [$\cdot 10^{-12}$ m$^2 \cdot$ s$^{-1}$] |
|---|---|---|---|---|---|---|
| M1-OPC | 1 | 25 | 66.5 | 24 | 15.9 | 8.71 |
| | 2 | | | | 14.8 | 8.03 |
| | 3 | | | | 16.3 | 8.94 |
| M2-GGBS | 1 | 30 | 40.3 | 24 | 11.7 | 5.15 |
| | 2 | | | | 12.4 | 5.47 |
| | 3 | | | | 10.9 | 4.76 |
| M3-FA | 1 | 25 | 69.8 | 24 | 20.9 | 11.50 |
| | 2 | | | | 20.0 | 10.96 |
| | 3 | | | | 20.9 | 10.99 |
| M4-SF | 1 | 50 | 15.2 | 24 | 10.3 | 2.72 |
| | 2 | | | | 8.3 | 2.17 |
| | 3 | | | | 9.8 | 2.58 |

with detecting the colour change boundary, and hence evaluating the penetration depth $x_d$, increases when the penetration depth is low or when the original colour of concrete is dark [13] (especially for the addition of GGBS). The pictures presented in Fig. 4 were taken with an artificial light source (flash light), in order to improve the contrast and consequently to improve the accuracy of the measurement. As can be observed in Fig. 4, the obtained chloride penetration fronts are with a clear colour change boundaries for all the analysed samples, relatively straight and not distorted. Subsequently, an average chloride penetration depth $x_d$ is measured and used for the calculation of $D_{RCM}$ (Eq. (2)), as reported in Table 6. It may be observed that the chloride diffusion coefficients for mortars M2-GGBS and M4-SF are reduced compared to the two other mortars, and this can be attributed to the microstructural changes induced by the filler effect and pozzolanic reaction. Thus, the permeability of these mortars is greatly reduced and the chloride ingress resistance is improved. The efficiency of pozzolanic additions to reduce the chloride ingress is also indicated in the total chloride concentration profile, as presented in Fig. 5. The results show that the chloride penetration depth $x_d$ in mortar M3-FA is greater in comparison to M1-OPC mortar (for these two mixtures the same voltage was applied). This may be presumably related to the slower course of the pozzolanic reaction of FA in comparison with mortars containing GGBS and SF. Therefore, further reduction of chloride diffusion coefficient $D_{RCM}$ is expected for M3-FA mortar in the course of the time.

The literature shows that the initial current value measured in the RCM test (at 30 V) may be correlated with the $D_{RCM}$ values [14,33]. The initial current depends mainly on the chemistry of pore solution and pore structure of concrete [14]. The initial current measured at 30 V was 69.8 mA for M3-FA mortar, 40.3 mA for M2-GGBS mortar and only 15.2 mA for M4-SF mortar. When the $D_{RCM}$ is plotted against the initial current, a linear relationship can be found, as is presented in Fig. 6. In the investigated range of voltages, this linear relationship is clear ($R^2 = 0.9092$).

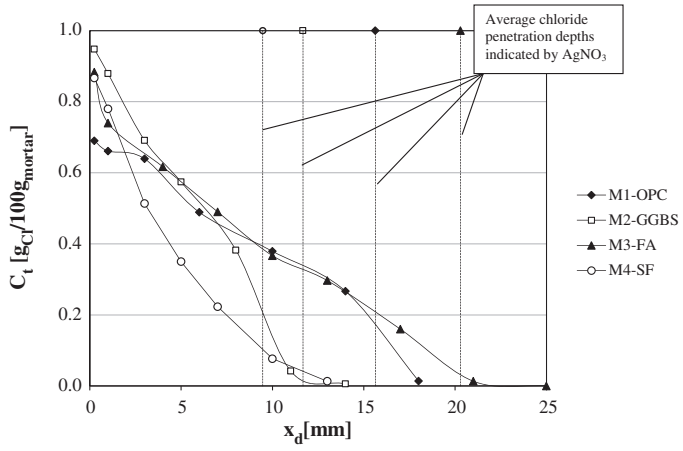


**Fig. 5.** Total chloride concentration profiles measured after the RCM test.

### 3.4. Total chloride concentration at the $AgNO_3$ colour change boundary

The chloride content at the colour change boundary is often expressed as % by the mass of concrete or as % by the mass of cement [5,8,10–13,15,18] because it is difficult to reliably measure the free chloride concentration profile in concrete. Theoretically, for a chloride contaminated concrete, only the chloride in pore solution can react with silver ions and yield the white precipitation. Nevertheless, for comparison purposes, the chloride content obtained in this study is expressed as % by the mass of mortar. This value multiplied by a dry density (see Table 5) over the binder volume in 1 m$^3$ (see Table 3) yields the total chloride content expressed as % by the mass of binder. Many researchers have measured the chloride concentration at the colour change boundary with OPC, but obtained very different results. Several factors such as the alkalinity of mortar, sprayed volume and concentration of $AgNO_3$ solution, pore solution volume, sampling method and methods used for measuring the free chloride concentration in concrete, as well as mix composition can be responsible for the high variability [19].

The total chloride concentrations at the chloride penetration depths $x_d$ have been determined here from the experimental profiles, as shown in Fig. 5. The depths, at which the colourimetric indicator displays the colour change, have been also plotted in Fig. 5, indicated as vertical lines. Fig. 5 shows that all the chloride concentration profiles in mortars after the RCM test decrease gradually from high values at the exposed surface to zero in deeper layers. The GGBS- and FA-mortars display a lower total chloride concentration in comparison to the OPC-mortar. This finding is in agreement with the fact that OPC-FA blends are known for a higher binding capacity in comparison to OPC based materials [34]. A higher binding capacity has been observed as well in mixes including GGBS [35]. The values of the total chloride concentration in concrete corresponding to the $AgNO_3$ detection boundary are summarized in Table 7 for all the samples analysed in this study. Table 7 shows that the total chloride concentration values range from 0.01 to 0.18% by the mass of concrete. Based on the work of Andrade et al. [12], the SF-based mortar should have the lowest chloride concentration at the colour change boundary and OPC-based mortar the highest concentration. This is confirmed in Table 7. The comparison between the total chloride concentrations at the colour change boundary for OPC-mortar obtained in this study and published in the literature is presented in Table 8. Otsuki et al. [10] proposed to use silver nitrate solute to determine the chloride penetration depth and quantified the chloride concentration at the colour change boundary. They found the total chloride content at the colour change boundary 0.15% by mass of cement

(which is equal to 0.08% by mass of concrete calculated from Otsuki's data). Baroghel-Bouny et al. [13] reported that the total chloride content for OPC concrete varied from 0.037–0.104% by the mass of concrete. Yuan et al. [8] reported the range between 0.028 and 0.207% by mass of concrete and Meck et al. [11] showed the range of the total chloride content at the colour change boundary for OPC concretes from 0.02 to 0.23%. Andrade et al. [12] found the average total chloride concentration at the colour change boundary of 0.18% for concrete made with different types of binders, which is very comparable to the data reported elsewhere [10–13,18].

From Figs. 4, 5 and Table 7 it can be found that the $AgNO_3$ method allows the detection of the chloride penetration front for mortars with SCM and the total chloride concentration, but the colour change boundary is different for the investigated binders. The results presented in Table 7 show that $AgNO_3$ colourimetric method is even more accurate in detecting the chloride penetration depth for mixtures incorporating SCM, compared to the OPC-based mortar, as the total chloride concentrations at the colour change boundary are much lower. Therefore, the $D_{RCM}$ for blended cement mortars is calculated for the accurate chloride penetration front, which is not affected by chloride binding. Therefore, Eq. (9) holds also for mortars based on the supplementary cementitious materials, as will be explained in the following section.

### 3.5. Extended chloride transport model

Based on the experimental total chloride concentration profiles obtained after performing the RCM test (Fig. 5), the values of the chloride effective coefficient $D_{eff}$, the mass transfer coefficient $k$, the binding capacity $K_b$ and the intensity of binding $n$ are optimized using a similar routine as presented by Spiesz et al. [16]. In such optimization process, the difference between the experimentally determined chloride concentration profile and the chloride profile computed from Eqs. (6) and (7) is minimized by adjusting the values of the above mentioned parameters. The values of the optimized parameters for OPC and blended cement mortars are shown in Table 9. Examples of the simulated total chloride concentration profiles for the investigated mortars are shown in Fig. 7. All the optimized chloride profiles are presented in the Appendix. From the presented results it can be seen that when replacing cement with 40% of GGBS (M2-GGBS), the binding capacity $K_b$ is increased. This indicates that the hydration products of M2-GGBS mortar are capable of binding more chlorides compared to the plain OPC-mortar (either chemically or physically, by the finer CSH gel). The same trend can be seen in the case of the 15% replacement of OPC by fly ash (M3-FA). On the other hand, when 10% of cement is replaced with silica fume (M4-SF), the binding capacity is slightly reduced, as is shown in Table 9. The optimized values of binding intensity $n$ are found in the range 0.49–0.53 for blended cement mortars. For OPC mortar (M1-OPC) the value of $n$ equals to 0.52–0.53, which is in line with the experimental values presented in [5] for an OPC mortar. In order to account for free and bound chloride concentration non-equilibrium, the mass transfer coefficient $k$ is introduced. The mass transfer coefficient $k$ is a parameter that plays a decisive role on the shape of the profile. When chlorides are bound faster (higher values of $k$), they do not have much freedom to penetrate deeper in to the mortar, which results in more abrupt chloride profile, as shown in the case of GGBS- and SF-based mortars (Fig. 7). The more gradual shape can be seen in M1-OPC and M3-FA mortar (Fig. 7), which is reflected by lower $k$ values, as found in Table 9.

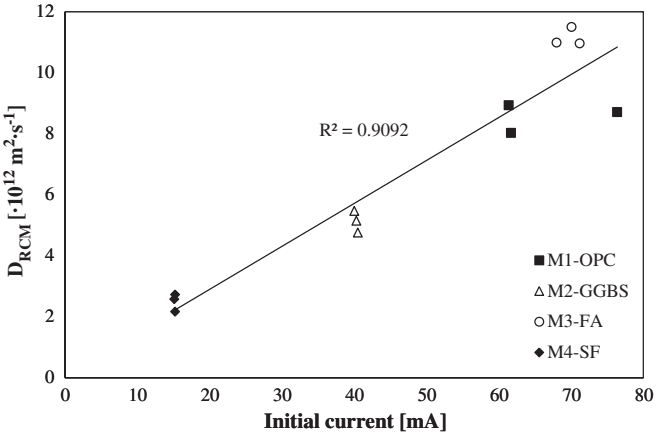


**Fig. 6.** Relationship between initial current and chloride diffusion coefficient $D_{RCM}$.

**Table 7**
Total chloride concentration at the $AgNO_3$ colour change boundary.

| Mortar mixture | Total chloride concentration by mass of concrete [%] |
|---|---|
| M1-OPC | 0.17–0.18 |
| M2-GGBS | 0.01–0.02 |
| M3-FA | 0.03–0.04 |
| M4-SF | 0.10–0.11 |

Table 9 shows that the values of the $D_{RCM}$ calculated from the basic RCM model (from the measured chloride penetration front) are similar to the values of the $D_{RCM}^*$ obtained from the extended model, following Eq. (9). It can be stated that the $D_{RCM}^*$ equals to the $D_{eff}/\phi$, as there is no chloride binding at the location of the chloride penetration front ($\partial c_b/\partial c \approx 0$) detected by $AgNO_3$ colourimetric method. A clear correlation between the chloride diffusion coefficients obtained from the colourimetric method and extended model can be seen also in Fig. 8. The good correlation demonstrates that the chloride penetration front in blended cement mortars can be accurately detected by using the spraying $AgNO_3$ colourimetric method and the chloride diffusion coefficient can be reliably obtained with the RCM test.

### 3.6. Relation between the chloride diffusion coefficients obtained from accelerated and non-accelerated tests

From Fig. 10 it can be seen that the total chloride concentration profiles are very similar for the three mortars (M1-OPC, M2-GGBS, M4-SF) after the natural chloride diffusion test, whereas a higher chloride penetration depth is observed in mortar M3-FA. Table 10 presents the chloride diffusion coefficients obtained following the accelerated RCM test ($D_{RCM}$) and the long-term diffusion test ($D_{app}$). It can be seen that the results obtained from the RCM test are generally higher than the results from the diffusion test, and they are well correlated linearly, as is presented in Fig. 9 for the individual results. This is consistent with the results obtained by other researchers [13,14]. The $D_{RCM}$ coefficients found in this study are about 35% higher than the $D_{app}$ obtained in the long-term diffusion test and both follow the same trend. Similar differences

**Table 8**
Total chloride concentration at the $AgNO_3$ colour change boundary for OPC-based concrete reported in the literature.

| Reference | Total chloride concentration by mass of concrete [%] |
|---|---|
| This study | ~0.18 |
| Yuan et al. [14] | 0.028–0.207 |
| Meck et al. [11] | 0.02–0.23 |
| Andrade et al. [12] | 0.06–0.17 |
| Otsuki et al. [10] | ~0.08[a] |
| Baroghel-Bouny et al. [13] | 0.037–0.104 |

[a] Calculated from Otsuki's data.

**Table 9**
Parameters optimized from the extended model.

| Mortar mixture | k [$\cdot 10^6$ l $\cdot$ s$^{-1}$] | $K_b$ [$\cdot 10^4$ dm$^{3n}$/g$^n$] | n [–] | $D_{eff}$ [$\cdot 10^{12}$ m$^2$ $\cdot$ s$^{-1}$] | $x_d$ [mm] | $D_{RCM}$ [$\cdot 10^{12}$ m$^2$ $\cdot$ s$^{-1}$] | $D_{RCM}^*$ [$\cdot 10^{12}$ m$^2$ $\cdot$ s$^{-1}$] |
|---|---|---|---|---|---|---|---|
| M1-OPC1 | 1.50 | 6.30 | 0.52 | 1.41 | 15.9 | 8.71 | 9.52 |
| M1-OPC2 | 1.63 | 6.35 | 0.53 | 1.37 | 14.8 | 8.03 | 9.55 |
| M1-OPC3 | 1.55 | 6.30 | 0.53 | 1.39 | 16.3 | 8.94 | 9.62 |
| M2-GGBS1 | 3.99 | 8.40 | 0.49 | 0.88 | 11.7 | 5.15 | 5.89 |
| M2-GGBS2 | 3.97 | 8.20 | 0.50 | 0.87 | 12.4 | 5.47 | 6.05 |
| M2-GGBS3 | 4.09 | 8.40 | 0.49 | 0.86 | 10.9 | 4.76 | 5.84 |
| M3-FA1 | 1.40 | 6.50 | 0.52 | 1.83 | 20.9 | 11.50 | 10.47 |
| M3-FA2 | 1.35 | 6.35 | 0.51 | 1.70 | 20.0 | 10.96 | 9.43 |
| M3-FA3 | 1.53 | 6.55 | 0.51 | 1.59 | 20.0 | 10.99 | 9.47 |
| M4-SF1 | 2.30 | 6.05 | 0.53 | 0.51 | 10.3 | 2.73 | 2.87 |
| M4-SF2 | 1.73 | 6.25 | 0.53 | 0.45 | 8.3 | 2.17 | 2.49 |
| M4-SF3 | 2.06 | 6.00 | 0.50 | 0.46 | 9.8 | 2.58 | 2.70 |

were presented in [14,33] who obtained the $D_{RCM}$ about 30% higher then $D_{app}$. The $D_{app}$ lower than $D_{RCM}$ can be explained by the age of samples upon the test period, i.e. 28 days for the RCM test and a period between 28–120 days for the long-term diffusion test. Therefore, a further microstructural densification of the mortars in that period is expected.

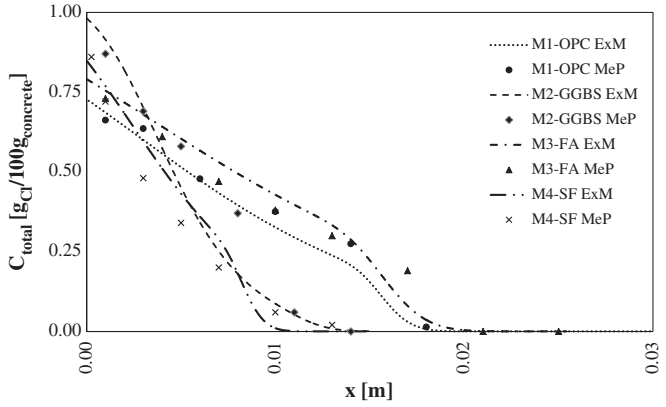


**Fig. 7.** Total chloride concentration profile for all mortars; MeP — measured profile, ExM — extended model.

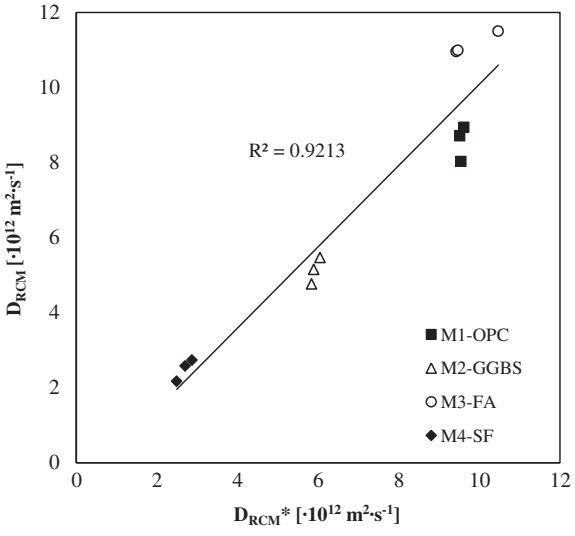


**Fig. 8.** Comparison of diffusion coefficients obtained from colourimetric method ($D_{RCM}$) and extended model ($D_{RCM}^*$).

## 4. Conclusions

Based on the presented investigations, the following conclusions can be drawn:

1. The reliability of the $AgNO_3$ colourimetric method to determine the chloride penetration depth is good for mortars based on different types of binders used in this study (GGBS, FA and SF). For the mixtures containing SCM additions, the total chloride concentration measured at the colour change boundary is even lower compared to the plain OPC mortar.
2. As the $AgNO_3$ colourimetric indicator allows reliable free-chloride penetration detection for mortars based on alternative binders, the $D_{RCM}$ calculated based on the true free-chloride penetration front is also correct. At the very low free-chloride concentration (i.e. the chloride penetration front) chloride binding is very limited during migration tests, so the $D_{RCM}$ remains unaffected by binding, which is reflected by a good correlation between the $D_{RCM}$ calculated from both, the basic and extended chloride transport models.
3. A linear correlation between the chloride diffusion coefficients obtained in accelerated and long-term diffusion tests is observed.

**Table 10**
Average chloride diffusion coefficients obtained from NT Build 492 and NT Build 443.

| Mortar mixture | $D_{RCM}$ [$\cdot 10^{12}$ m$^2$ $\cdot$ s$^{-1}$] | $D_{app}$ [$\cdot 10^{12}$ m$^2$ $\cdot$ s$^{-1}$] |
|---|---|---|
| M1-OPC | 8.56 | 5.94 |
| M2-GGBS | 5.13 | 3.66 |
| M3-FA | 11.15 | 7.21 |
| M4-SF | 2.49 | 1.96 |

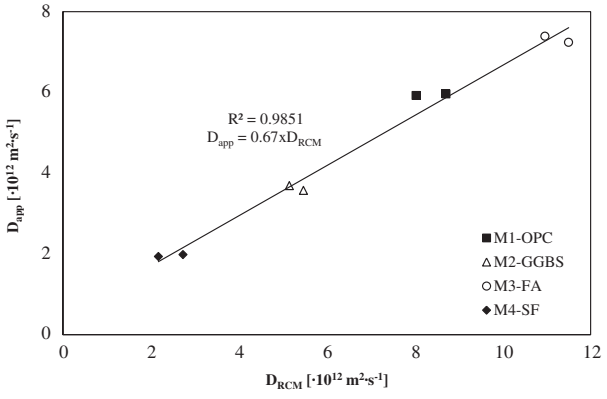


**Fig. 9.** Relationship between $D_{RCM}$ obtained from NT Build 492 and $D_{app}$ obtained from NT Build 443.

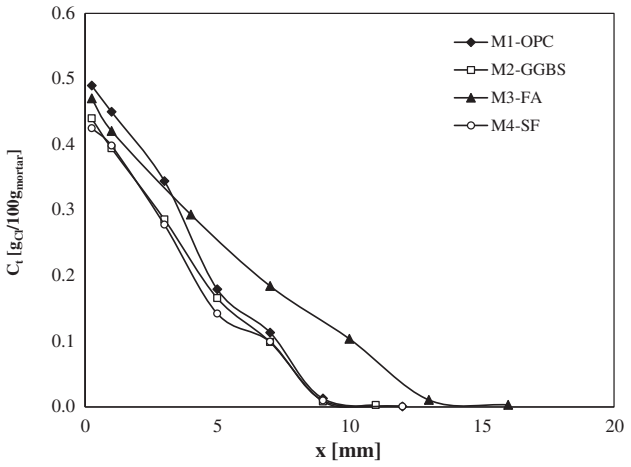


**Fig. 10.** Chloride profiles in blended cement mortars obtained after 120 days of bulk diffusion test (NT Build 443).

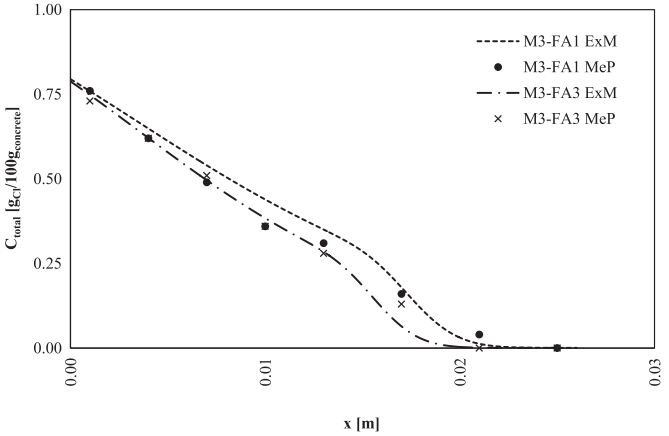


**Fig. 13.** Total chloride concentration profiles for mortars M3-FA1, M3-FA3.

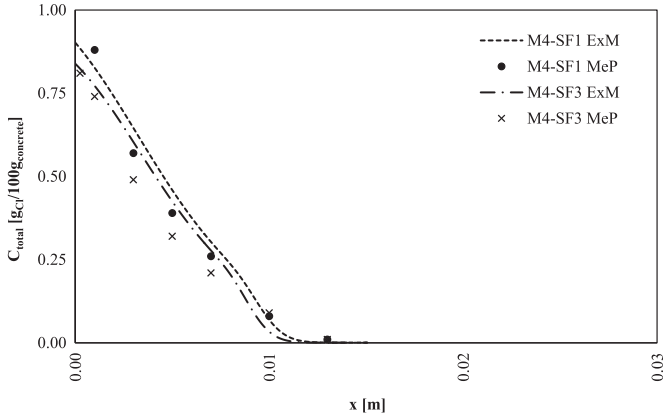


**Fig. 14.** Total chloride concentration profiles for mortars M4-SF1, M4-SF3.

## Appendix A

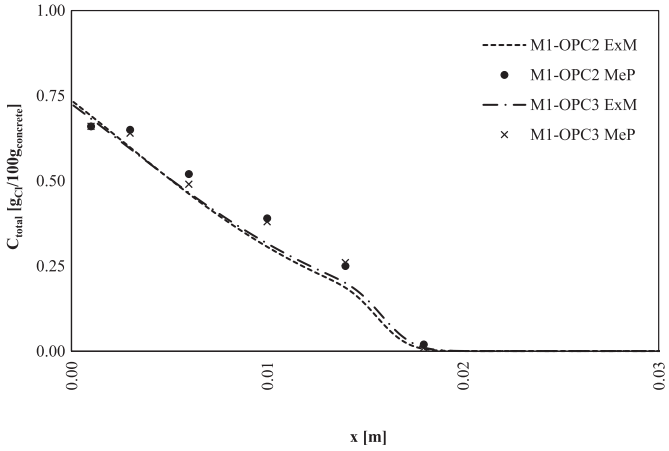


**Fig. 11.** Total chloride concentration profiles for mortars M1-OPC2, M1-OPC3.

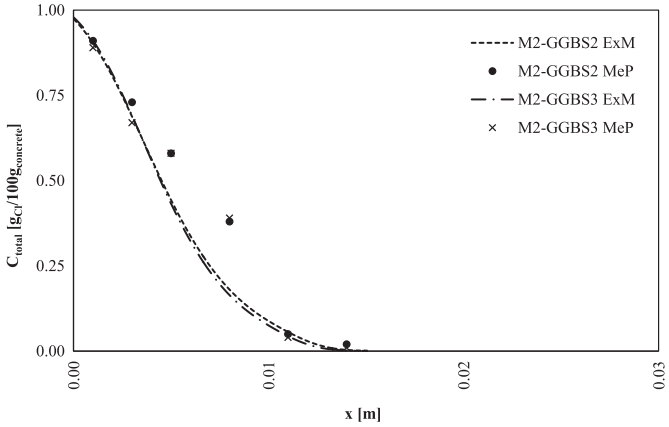


**Fig. 12.** Total chloride concentration profiles for mortars M2-GGBS2, M2-GGBS3.

## References

[1] N.S. Martys, C.E. Ferraris, Capillary transport in mortars and concrete, Cem. Concr. Res. 27 (5) (1997) 747–760.
[2] Q. Yuan, C. Shi, G. De Schutter, K. Audenaert, D. Deng, Chloride binding of cement-based materials subjected to external chloride environment — a review, Constr. Build. Mater. 23 (1) (Jan. 2009) 1–13.
[3] NT Build 443, Concrete, Hardened: Accelerated Chloride Penetration, 1995.
[4] ASTM C1556–03, Standard Test Method for Determining the Apparent Chloride Diffusion Coefficient of Cementitious Mixtures by Bulk Diffusion, vol. 042003 1–7.
[5] L. Tang, Chloride Transport In Concrete — Measurement And Prediction, Chalmers University of Technology, Goteborg, Sweden, 1996.
[6] NT Build 492, Concrete, Mortar and Cement-Based Repair Materials: Chloride Migration Coefficient from Non-Steady-State, Migration Experiments, 1999.
[7] P.E. Steicher, M.G. Alexander, "A critical evaluation of chloride diffusion test methods for concrete,", Proc. 3rd CANMET/ACI Int. Conf. Durab. Concr. Nice, Fr. vol. ACI SP-145 (1994) 517–530.
[8] Q. Yuan, C. Shi, F. He, G. De Schutter, K. Audenaert, K. Zheng, Effect of hydroxyl ions on chloride penetration depth measurement using the colorimetric method, Cem. Concr. Res. 38 (10) (Oct. 2008) 1177–1180.
[9] F. He, C. Shi, Q. Yuan, X. An, B. Tong, Calculation of chloride concentration at color change boundary of $AgNO_3$ colorimetric measurement, Cem. Concr. Res. 41 (11) (Nov. 2011) 1095–1103.
[10] N. Otsuki, S. Nagataki, K. Nakashita, Evaluation of the AgNO3 solution spray method for measurement of chloride penetration into hardened cementitious matrix materials, Constr. Build. Mater. 7 (4) (Dec. 1993) 195–201.
[11] E. Meck, V. Sirivivatnanon, Field indicator of chloride penetration depth, Cem. Concr. Res. 33 (8) (Aug. 2003) 1113–1117.
[12] C. Andrade, M. Castellote, C. Alonso, C. González, Relation between colourimetric chloride penetration depth and charge passed in migration tests of the type of standard ASTM C1202-91, Cem. Concr. Res. 29 (3) (Mar. 1999) 417–421.
[13] V. Baroghel-Bouny, P. Belin, M. Maultzsch, D. Henry, AgNO3 spray tests: advantages, weaknesses, and various applications to quantify chloride ingress into concrete. Part 1: Non-steady-state diffusion tests and exposure to natural conditions, Mater. Struct. 40 (8) (Apr. 2007) 759–781.
[14] Q. Yuan, Fundamental Studies on Test Methods for the Transport of Chloride Ions in Cementitious Materials, University Gent, Gent, 2009.

[15] M. Maes, E. Gruyaert, N. Belie, Resistance of concrete with blast-furnace slag against chlorides, investigated by comparing chloride profiles after migration and diffusion, Mater. Struct. 46 (1–2) (Jul. 2012) 89–103.
[16] P. Spiesz, M.M. Ballari, H.J.H. Brouwers, RCM: A new model accounting for the non-linear chloride binding isotherm and the non-equilibrium conditions between the free- and bound-chloride concentrations, Constr. Build. Mater. 27 (1) (Feb. 2012) 293–304.
[17] L. Tang, Electrically accelerated methods for determining chloride diffusivity in concrete — current development, Magazine of Concr. Res. vol. 48 (176) (1996) 173–179.
[18] Q. Yuan, D. Deng, C. Shi, G. Schutter, Application of silver nitrate colorimetric method to non-steady-state diffusion test, J. Cent. South Univ. 19 (10) (Oct. 2012) 2983–2990.
[19] F. He, C. Shi, Q. Yuan, C. Chen, K. Zheng, $AgNO_3$-based colorimetric methods for measurement of chloride penetration in concrete, Constr. Build. Mater. 26 (1) (Jan. 2012) 1–8.
[20] K.D. Stanish, The Migration of Chloride Ions in Concrete, University of Toronto, Canada, 2002.
[21] B. Šavija, M. Luković, E. Schlangen, Lattice modeling of rapid chloride migration in concrete, Cem. Concr. Res. 61–62 (Jul. 2014) 49–63.
[22] K. Stanish, R.D. Hooton, M.D.A. Thomas, A novel method for describing chloride ion transport due to an electrical gradient in concrete: Part 1. Theoretical description, Cem. Concr. Res. 34 (1) (Jan. 2004) 43–49.
[23] P. Spiesz, H.J.H. Brouwers, The apparent and effective chloride migration coefficients obtained in migration tests, Cem. Concr. Res. 48 (Jun. 2013) 116–127.
[24] A. Atkinson, a.K. Nickerson, The diffusion of ions through water-saturated cement, J. Mater. Sci. 19 (9) (1984) 3068–3078.
[26] EN 197–1, Cement. Composition, Specifications and Conformity Criteria for Common Cements, 2011.
[27] EN 196–1, Methods of Testing Cement. Determination of Strength, vol. 32005.
[28] P. Spiesz, H.J.H. Brouwers, Influence of the applied voltage on the Rapid Chloride Migration (RCM) test, Cem. Concr. Res. 42 (8) (Aug. 2012) 1072–1082.
[29] ASTM C642-97, "Standard Test Method for Density, Absorption, and Voids in Hardened Concrete" (1997) 4–6.
[30] G. Quercia, P. Spiesz, G. Hüsken, H.J.H. Brouwers, SCC modification by use of amorphous nano-silica, Cem. Concr. Compos. 45 (Jan. 2014) 69–81.
[31] R. Yu, P. Spiesz, H.J.H. Brouwers, Effect of nano-silica on the hydration and microstructure development of ultra-high performance concrete (UHPC) with a low binder amount, Constr. Build. Mater. 65 (Aug. 2014) 140–150.
[32] E.J. Garboczi, Permeability, diffusivity, and microstructural parameters: a critical review, Cem. Concr. Res. 20 (1990) 591–601.
[33] R. Loser, B. Lothenbach, A. Leemann, M. Tuchschmid, Chloride resistance of concrete and its binding capacity — comparison between experimental results and thermodynamic modeling, Cem. Concr. Compos. 32 (1) (Jan. 2010) 34–42.
[34] V.G. Papadakis, Effect of supplementary cementing materials on concrete resistance against carbonation and chloride ingress, Cem. Concr. Res. 30 (2) (2000) 291–299.
[35] R. Luo, Y. Cai, C. Wang, X. Huang, Study of chloride binding and diffusion in GGBS concrete, Cem. Concr. Res. 33 (1) (2003) 1–7.